UCSF
UC San Francisco Previously Published Works

Title
Impaired Potentiation of Theta Oscillations During a Visual Cortical Plasticity Paradigm in Individuals With Schizophrenia

Permalink
https://escholarship.org/uc/item/5nf8t2ks

Journal
FRONTIERS IN PSYCHIATRY, 11(SUPPL 1)

ISSN
1664-0640

Authors
Hamilton, Holly K
Roach, Brian J
Cavus, Idil
et al.

Publication Date
2020

DOI
10.3389/fpsyt.2020.590567

Peer reviewed

Impaired Potentiation of Theta Oscillations During a Visual Cortical Plasticity Paradigm in Individuals With Schizophrenia

Holly K. Hamilton [1,2], Brian J. Roach [1,3], Idil Cavus [4], Timothy J. Teyler [5], Wesley C. Clapp [6], Judith M. Ford [1,2], Erendiz Tarakci [1,3], John H. Krystal [4] and Daniel H. Mathalon [1,2*]

[1] San Francisco Veterans Affairs Health Care System, San Francisco, CA, United States, [2] Department of Psychiatry and Behavioral Sciences, Weill Institute for Neurosciences, University of California, San Francisco, San Francisco, CA, United States, [3] Northern California Institute for Research and Education, San Francisco, CA, United States, [4] Department of Psychiatry, Yale University, New Haven, CT, United States, [5] WWAMI Medical Education Program, University of Idaho, Moscow, ID, United States, [6] Neuroscouting, LLC, Somerville, MA, United States

Long-term potentiation (LTP) is a form of experience-dependent synaptic plasticity mediated by glutamatergic transmission at N-methyl-D-aspartate receptors (NMDARs). Impaired neuroplasticity has been implicated in the pathophysiology of schizophrenia, possibly due to underlying NMDAR hypofunction. Analogous to the high frequency electrical stimulation used to induce LTP *in vitro* and *in vivo* in animal models, repeated high frequency presentation of a visual stimulus in humans *in vivo* has been shown to induce enduring LTP-like neuroplastic changes in electroencephalography (EEG)-based visual evoked potentials (VEPs) elicited by the stimulus. Using this LTP-like visual plasticity paradigm, we previously showed that visual high-frequency stimulation (VHFS) induced sustained changes in VEP amplitudes in healthy controls, but not in patients with schizophrenia. Here, we extend this prior work by re-analyzing the EEG data underlying the VEPs, focusing on neuroplastic changes in stimulus-evoked EEG oscillatory activity following VHFS. EEG data were recorded from 19 patients with schizophrenia and 21 healthy controls during the visual plasticity paradigm. Event-related EEG oscillations (total power, intertrial phase coherence; ITC) elicited by a standard black and white checkerboard stimulus (∼0.83 Hz, several 2-min blocks) were assessed before and after exposure to VHFS with the same stimulus (∼8.9 Hz, 2 min). A cluster-based permutation testing approach was applied to time-frequency data to examine LTP-like plasticity effects following VHFS. VHFS enhanced theta band total power and ITC in healthy controls but not in patients with schizophrenia. The magnitude and phase synchrony of theta oscillations in response to a visual stimulus were enhanced for at least 22 min following VHFS, a frequency domain manifestation of LTP-like visual cortical plasticity. These theta oscillation changes are deficient in patients with schizophrenia, consistent with hypothesized NMDA receptor dysfunction.

Keywords: schizophrenia, cortical plasticity, long-term potentiation, neural oscillations, theta band, electroencephalography

INTRODUCTION

Neural plasticity dysfunction in schizophrenia has been hypothesized to underlie cognitive impairment (1–3), which is a core feature of the illness and a major determinant of functional outcomes (4, 5). Long-term potentiation (LTP) is a basic mechanism of experience-dependent synaptic plasticity that produces enduring enhancement of synaptic transmission (6, 7) and is widely considered to be the leading candidate cellular mechanism of learning and memory (7–10). Importantly, the most common form of LTP is known to be dependent on glutamatergic neurotransmission at N-methyl-D-aspartate receptors (NMDARs) (11, 12). Converging evidence from genetic (13), pharmacological (14–16), post-mortem (17), and neuroreceptor imaging (18) studies support NMDAR hypofunction as a key pathophysiological process in schizophrenia (19, 20). Based on this NMDAR hypofunction model, NMDAR-dependent forms of synaptic plasticity, including LTP, are theorized to be deficient in schizophrenia (1–3, 21, 22).

Several lines of evidence suggest that the pathophysiology of schizophrenia involves altered synaptic plasticity. First, genetic abnormalities associated with schizophrenia risk have been implicated in the regulation of synaptic plasticity (23, 24). Expression of these risk genes in animal models results in NMDAR hypofunction and impaired LTP (25), while NMDAR inhibition in animals is associated with deficient LTP (26, 27). Furthermore, post-mortem studies have shown that schizophrenia is associated with reduced neuropil [see (28)] and dendritic spine density [see (29)] that are normally generated and maintained through mechanisms of experience-dependent synaptic plasticity, and multiple possible pathophysiological pathways have been identified that could contribute to both deficient plasticity and reduced dendritic spine density (29). However, direct evidence of deficient LTP in schizophrenia has been limited until recently due to a lack of translational methods for assessing LTP in humans *in vivo*.

In animal studies, LTP is typically observed following high frequency "tetanizing" electrical stimulation and is identified electrophysiologically as a persistent increase in postsynaptic cellular currents using single-cell or local field recordings. Using these methods, LTP has been documented in animals at synapses in regions that include the hippocampus, amygdala, and striatum, as well as visual, auditory, and somatosensory cortices (9, 10, 30). In rodents, LTP in visual cortex can also be induced by repeated visual sensory stimulation (31–34), such that repeated presentations of visual line-grating stimuli induce persistent increases in the strength of the visual evoked potential (VEP) cortical responses to those stimuli. Importantly, repeated exposure to visual stimuli induces a form of plasticity that has the cardinal cellular and molecular features of synaptic LTP [see (34)]. Accordingly, these forms of sensory plasticity are thought to represent an endogenous form of sensory LTP subserving perceptual learning (34).

Based on the animal studies of LTP described above, paradigms for examining sensory LTP *in vivo* in humans have recently been developed (7, 35, 36). These paradigms are similar to the tetanizing electrical and visual stimulation paradigms used in rodents and involve repeated presentation of a sensory stimulus to induce LTP-like plasticity in the corresponding sensory cortex (36). Potentiation of the visual cortical response induced by these paradigms has been documented primarily using scalp-recorded electroencephalography (EEG)-based VEPs (35, 37–40), but also with functional magnetic resonance imaging (41, 42) and behavioral performance (36, 43) measures. Notably, the plasticity induced in human sensory cortex by these sensory stimulation paradigms conforms to several rules of synaptic LTP, including potentiation by stimulation (36, 38, 43), persistence of plasticity effects (36, 38), input specificity (minimal or no potentiation of a non-tetanized control stimulus) (39, 40, 43, 44), temporal and spatial specificity (e.g., only VEP components in specific time windows with specific cortical topographies are potentiated) (36, 39, 40, 45), and NMDAR dependency (46, 47).

Using various sensory stimulation paradigms, several studies have documented impaired LTP-like plasticity in schizophrenia (45, 48), as well as in individuals at clinical high risk for developing a psychotic disorder (Jacob et al., under review) and in bipolar II disorder (49–51) and major depressive disorder (52). Previously, we showed that visual high frequency stimulation (VHFS; ~8.9 Hz) induced sustained (enduring for at least 22 min post-VHFS) potentiation of visual N1b and C1 VEP amplitudes in healthy individuals but not in patients with schizophrenia (45). We also observed schizophrenia patients and healthy controls to have comparable attention-modulated visual steady state responses (VSSRs) entrained to the frequency and phase of the VHFS. However, greater VHFS-driven VSSRs predicted greater N1b potentiation in healthy individuals but not in schizophrenia patients, suggesting that the observed VEP plasticity impairment in schizophrenia patients was not due to deficient attention during visual stimulation, but rather dysfunction of the neural mechanisms that support plasticity.

Synchronized neural oscillations are involved in plasticity of cortical networks, modulating the precise relative spike timing that is critical for synaptic plasticity, and are known to play a crucial role in plasticity mechanisms such as LTP (53–56). Neural assemblies show synchronous oscillatory activity across a wide range of frequency bands (e.g., delta, theta, alpha, beta, gamma), observed both in local field potentials as well as in scalp-recorded EEG. These oscillations are implicated as a primary mechanism for coordinated communication between local and distant neuronal networks and are involved in the integration of a variety of brain functions including learning and memory as well as other sensory, perceptual, and higher-order cognitive processes. Compromise of the mechanisms that subserve neural oscillations and their synchronization has been implicated in schizophrenia [e.g., see (57, 58)]. Along with hypothesized dysfunctional LTP, deficiencies in these mechanisms may render event-related neural oscillations and their synchronization less susceptible to modification by experience. Moreover, evidence from rodent studies documents that successful LTP depends on a transient suppression of EEG theta power during tetanization and a correlated increase in theta and gamma power immediately following tetanization (59, 60), suggesting that dysfunction of the mechanisms that generate and

synchronize neural oscillations could contribute to compromised LTP in schizophrenia.

While sensory neuroplasticity studies have primarily measured evoked potentials as indices of LTP-like plasticity, we are aware of only one study to date that examined the effect of a visual tetanus on neural oscillations. Clapp et al. (61) tested whether VHFS affected the event-related desynchronization (ERD) of the alpha rhythm, which is a measure of the event-related decrease in oscillatory power across trials irrespective of signal phase (62) reflecting the release from cortical inhibition and the active engagement of cortical networks during stimulus processing or cognitive performance (63). Delivery of VHFS resulted in a significant increase in alpha ERD in response to the presented visual stimulus that persisted for 1 h in a sample of healthy individuals (61).

Here, we extend our prior work by conducting a time-frequency analysis of our prior data published in the EEG time domain as VEPs (45), using established spectral decomposition methods (64) to test the hypotheses that (1) plasticity effects of repeated visual stimulation extend beyond the phase-locked VEP to frequency-specific oscillatory activity, and (2) these plasticity effects are compromised in schizophrenia. Given the novelty of applying time-frequency analyses to EEG data collected during the visual LTP-like plasticity paradigm, we made no assumptions about which frequency bands, time windows, or scalp locations would show plasticity effects. Instead, we used an unbiased, data-driven, cluster-based permutation testing approach described previously (65) in order to identify significant spatio-temporal clusters within specific frequency bands showing differential plasticity effects between patients and controls. Once significant clusters were identified, we then compared the plasticity effects in each group in the identified clusters. In addition to oscillatory total power (calculated from the stimulus-locked single trial EEG epochs), we examined inter-trial coherence (ITC) of phase, which assesses phase consistency of frequency-specific neural oscillations with respect to visual stimulus onset across trials (66). Moreover, we asked whether spatio-temporal clusters showing total power or ITC plasticity effects were associated with the VEP plasticity effects and VSSR measures from our previous report (45). Finally, we sought to replicate Clapp et al.'s (61) finding of VHFS-induced alpha ERD enhancement in healthy individuals, and we examined whether patients with schizophrenia showed deficient potentiation of alpha-ERD following VHFS.

MATERIALS AND METHODS

Participants

Participants were 19 patients with schizophrenia and 21 healthy controls (HC) from a previous report (45) that examined VEP measures of LTP-like plasticity induced by VHFS. All participants were evaluated using the Structured Clinical Interview for DSM-IV (67). Participants with schizophrenia met DSM-IV criteria and were recruited from local community clinics. Symptoms were rated using the Positive and Negative Syndrome Scale (PANSS) (68) within 2 weeks of EEG recording. HC participants were recruited from the local community and had no history of any major DSM-IV Axis I disorder and had no first-degree

relatives with a diagnosis of schizophrenia or bipolar disorder. Participants were excluded if they had a history of substance abuse or benzodiazepine use within 30 days prior to study enrollment, history of alcohol or substance dependence (except nicotine), neurological or medical illness compromising the central nervous system, head injury with loss of consciousness, and left-handedness based on a quantitative scale (69). All participants had normal or corrected-to-normal vision. The schizophrenia and HC groups did not differ in age and parental socioeconomic status (70). All participants provided written informed consent and the study was approved by the West Haven VA and Yale University Institutional Review Boards.

Experimental Paradigm

The paradigm, which was previously described in detail (45) and modified from Teyler et al. (38), involved recording of EEG during baseline and post-VHFS assessment blocks. While focusing on a central fixation cross, participants viewed the visual stimuli shown centrally on a white background on a 15-inch LCD monitor (800 × 600 pixels with a 60 Hz refresh rate) located 57 cm in front of them. Each 2-min assessment block consisted of a pseudorandom oddball sequence with 90% standard black and white checkerboard circle stimuli to assess plasticity effects (8 cm in diameter, subtending 8° of visual angle, each check subtending 0.3°) and 10% target blue and white checkerboard square stimuli to maintain attention to the visual task (9 × 9 cm, subtending 9° of visual angle, each check subtending 0.5°) presented at ∼0.83 Hz (1,216 ms mean stimulus onset asynchrony (SOA), range 1,075–1,340 ms). This presentation rate was chosen to be below the 1 Hz rate previously shown to induce VEP depotentiation (38). To monitor attention, participants were asked to respond to the target stimulus by pressing a button with their right hand. As reported previously, the schizophrenia and HC groups performed similarly in their response accuracy to target stimuli (45).

The 2-min VHFS block, designed to induce potentiation, consisted of the repeated presentation of the standard circular checkerboard at ∼8.87 Hz (113 ms mean SOA, range 99–116 ms), at a rapid flicker rate below the perceptual fusion threshold (38).

VEP assessment blocks were administered at 4 and 2 min prior to VHFS (Baseline-1 and Baseline-2) and 2, 4, and 20 min after VHFS (Post-1, Post-2, and Post-3). An unrelated auditory task was performed in the interval between the Post-2 and Post-3 assessment blocks.

EEG Acquisition and Processing

EEG was recorded during the VHFS plasticity paradigm using a 32-channel Neuroscan Synamps amplifier (Compumedics, Charlotte, NC) with data acquired continuously (0.5–200 Hz bandpass filter; 1,000 Hz digitization rate) from 29 Ag/AgCl sintered electrodes (EasyCap, Munich, Germany). A linked mastoid reference and a forehead (FPz) ground were used. Electro-oculograms were recorded horizontally (HEOG) from the outer canthi of the eyes and vertically (VEOG) from above and below the right orbit. Impedances did not exceed 10 kΩ.

Data were analyzed using Brain Vision Analyzer (Brain Products, Munich, Germany) and custom MATLAB

(MathWorks, Natick, MA) scripts. Continuous data were high-pass filtered at 1 Hz (24 dB/octave) and 3 s (-1 to 2 s) epochs were extracted, time-locked to the onsets of the standard checkerboard stimulus. After ocular artifact correction (71), epochs were re-referenced to Fz and baseline-corrected using the 100 ms pre-stimulus baseline. Next, the single trial data were cleaned of muscle artifacts with blind source separation using canonical correlation analysis (BSS-CCA) similar to the method described by others (72, 73) and as we have used previously (74). Outlier trials were rejected and then outlier electrodes were interpolated within single trial epochs based on previously established criteria (75). A spherical spline interpolation (64) was applied to any channel that was determined to be a statistical outlier ($|z| > 3$) on one or more of four parameters, including variance to detect additive noise, median gradient to detect high-frequency activity, amplitude range to detect pop-offs, and deviation of the mean amplitude from the common average to detect electrical drift. The median number of trials rejected per block was three in both HC and schizophrenia groups. EEG data from one of the 22 HC participants included in the prior report (45) were excluded from the present analysis because single trial data were lost.

Time-Frequency Analysis

Single-trial EEG epochs time-locked to the standard checkerboard stimulus were analyzed with a complex Morlet wavelet decomposition using a freely distributed FieldTrip toolbox (76) in MATLAB. Specifically, we used a Morlet wavelet with a Gaussian shape defined by a ratio (σ_f = f/C) and $6\sigma_t$ duration [f is the center frequency and $\sigma_t = 1/(2\psi_f)$]. In a classic wavelet analysis, C is a constant, ensuring an equal number of cycles in the mother wavelet for each frequency. Such an approach was used to create wavelets for this analysis, and C was set to seven. In this approach, as the frequency (f) increases, the spectral bandwidth ($6\sigma_f$) increases. As such, center frequencies were set to minimize spectral overlap, resulting in 10 frequency bins: 3, 5, 7, 10, 14, 20, 28, 40, 56, and 79 Hz. ITC was then calculated as 1 minus the circular phase angle variance, as previously described (66). ITC provides a measure of the phase consistency of frequency specific oscillations with respect to stimulus onset across trials on a millisecond basis. Total power was calculated by averaging the squared single trial magnitude values in each frequency bin on a millisecond basis. Following a 25% trimmed-means averaging approach, power values were $10\log_{10}$ transformed and then baseline corrected by subtracting the mean of the pre-stimulus baseline (-200 to -100 ms) from each time point separately for every frequency. The resulting values describe change in total power relative to baseline in decibels (dB).

Statistical Analysis
Non-parametric, Cluster-Based Permutation Testing
A cluster-based permutation testing approach was applied to time-frequency data in two stages. LTP-like plasticity effects were defined as pre- vs. post-VHFS changes in the time-frequency maps, where pre-VHFS was the average of the first two baseline blocks and post-VHFS was the final assessment

block, which occurred 20 min following VHFS. Testing for group differences in this LTP-like plasticity effect is equivalent to an interaction effect of group (schizophrenia vs. HC) × time (pre- vs. post-VHFS) in an analysis of variance model. However, this interaction effect was formulated as an independent samples t-test to facilitate permutation tests by calculating contrast or difference maps (e.g., (Post-3 ITC) – [(Baseline-1 + Baseline-2 ITC)/2]). These difference maps from 15 parietal-occipital electrodes nearest to POz (P7, P5, P3, Pz, P4, P6, P8, PO3, POz, PO4, PO9, PO7, Oz, PO8, and PO10) for each subject were down-sampled to 250 Hz to reduce the number of time points tested, and they were limited to the period of the epoch from 0 to 500 ms. These time-frequency difference maps served as input to the permutation test procedure.

Cluster-based permutation tests of EEG data have been described previously (65), but the setup along with specific parameters for this analysis should be described. First, independent samples t-test statistics are calculated for every time sample and electrode (N_{times} = 125 * $N_{frequencies}$ = 10 * $N_{electrodes}$ = 15, yielding 18,750 t statistics). All test statistics that failed to reach statistical significance at an uncorrected 0.05, two-tailed alpha level (i.e., any test where $-2.024394 \leq t \leq 2.024394$) were ignored. All test statistics that survived this initial height-threshold were grouped into spatial-spectral-temporal clusters where clusters were defined by neighboring electrodes, frequencies, and/or time samples of statistically significant t statistics (note: a single time point that survived thresholding but had no significant neighbors is still considered a "cluster"). Spatial neighbors were defined based on a triangulation algorithm implemented in FieldTrip that attempts to construct triangles between nearby electrodes based on a two-dimensional projection of 3D electrode locations (76). All t statistics in each cluster were summed to determine the cluster statistic (or cluster "mass" t_{sum}). Such cluster statistics were similarly defined in 10,000 iterations where group membership was randomly permuted and all subjects were re-assigned to either HC or schizophrenia "groups" without replacement. On average, these permutations should cancel out any true group effects, leaving only clusters that arise by chance. The maximum absolute cluster statistic is saved from each of the 10,000 iterations and defines the positive tail of the null distribution of cluster statistics. The null distribution is assumed to be symmetric so that same set of cluster statistics is multiplied by-1 to define the negative tail of the null distribution. The p-value associated with each cluster statistic from the original data set was then determined based on its position in this null distribution, and any cluster with a $p <$ 0.05 was considered cluster-corrected, significant, controlling the family-wise error rate for multiple comparisons. This procedure was applied separately to ITC and total power values.

As these are tests of the Group × Time interaction effect and could miss main effects of time, a second set of permutation tests were run, ignoring group membership. In this set of tests, one-sample t-test statistics were calculated to determine if the time-frequency difference maps differed from zero, and cluster statistics were similarly defined in 10,000 iterations where the input data were flipped (i.e., multiplied by-1) for a randomly selected half of the participants. These tests were constrained to

only include those samples (of 18,750 total) that did not show significant group differences in the first set of tests.

Analysis

For any given cluster that showed a cluster-corrected Group × Time effect (cluster $p < 0.05$), the mean amplitude was calculated across the electrodes, frequencies, and times in the difference map associated with the cluster. These mean values were calculated separately for every subject and each of the assessment blocks, then used to determine the pattern of LTP-like plasticity differences between HC and schizophrenia participants. A mixed effects model analysis conducted in SAS v9.4 (PROC MIXED) was applied treating participant, nested within group, as a random factor, group as the between subjects factor, and time (Baseline, Post-1, Post-2, and Post-3) as a within-subjects repeated measure with four levels. Planned contrasts were used to examine the plasticity effects within each group. While we report the test of the Group × Time interaction effect to compare plasticity effects between groups based on the mean value of the cluster, it should be recognized that this test is applied to a cluster, the constituents of which already showed a significant Group × Time interaction in the cluster-based permutation testing. As such, the p-value for this Group × Time effect is somewhat inflated and should therefore simply be considered an expected confirmation of the cluster results. For the remaining mixed model effects tested, alpha was set to $p = 0.05$. For all models, the best-fitting variance-covariance structure was selected based on Schwartz-Bayesian Information Criterion [BIC (77)]. General linear models (GLMs) were also used to assess relationships between any significant cluster mean and measures from our previous report, including VHFS-driven VSSR and N1b VEP component post-VHFS minus pre-VHFS change scores (45).

Finally, we attempted to replicate the prior report of increased alpha total power ERD (61) following VHFS by taking the mean total power value in the 100–380 ms post-stimulus range relative to a −200 to 0 ms baseline at electrode Oz. Like the other mixed models, Group, Time, and Group X Time interaction effects were assessed.

RESULTS

Participant demographics and clinical characteristics are shown in **Table 1**.

Non-parametric, Cluster-Based Permutation Testing

There was one cluster showing a significant group difference in the ITC permutation test set (cluster-$p = 0.025$). This cluster spanned all electrodes but two (P7 and PO9), and while it encompassed delta (3 Hz) to theta (5–7 Hz) frequency bands, it was dominated by 5 Hz (theta) activity. The cluster spanned the 0–496 ms time window, and the peak test statistic occurred at 224 ms. As this is essentially a Group X Time interaction effect, plots of the mean ITC within this cluster from the five assessment blocks demonstrate the pattern of the effects in this cluster (see **Figure 1**). After omitting this cluster from the difference maps,

there were no clusters showing a main effect of Time (all cluster $p > 0.05$).

There was also one cluster showing a significant group difference in the total power permutation test set (cluster-$p = 0.033$). This cluster spanned all electrodes but P7, 0–450 ms (112 ms peak), and only included the 5 Hz (theta) frequency band. The pattern of effects in this cluster can be appreciated when cluster means are broken down by assessment block and group (see **Figure 2**). Like ITC, there were no clusters showing a main effect of Time in the subsequent permutation test set where this 5 Hz cluster was omitted (all cluster $p > 0.05$).

Analysis

Based on the BIC fit statistics, an auto-regressive (1) variance-covariance structure was the best choice for the mean ITC cluster model and a compound symmetry variance-covariance structure was selected for the mean total power cluster model. Mean ITC and total power cluster values are shown in **Table 2**.

ITC Cluster

Mean ITC did not differ between Baseline-1 and Baseline-2 in schizophrenia patients ($p = 0.79$) or in HCs ($p = 0.14$), so the baseline blocks were averaged for each participant to yield a single collapsed Baseline mean ITC value. Mean ITC at Baseline was slightly greater in schizophrenia patients than in HCs ($p = 0.045$). As expected from the analysis by which the cluster was identified, the mixed model of mean ITC showed a significant Group X Time interaction [$F_{(3,114)} = 9.02$, $p < 0.0001$] (see **Figure 1**). In HCs, VHFS enhanced mean ITC at post-VHFS blocks relative to Baseline (Post-1: $p = 0.0001$; Post-2: $p = 0.054$; Post-3: $p = 0.005$).
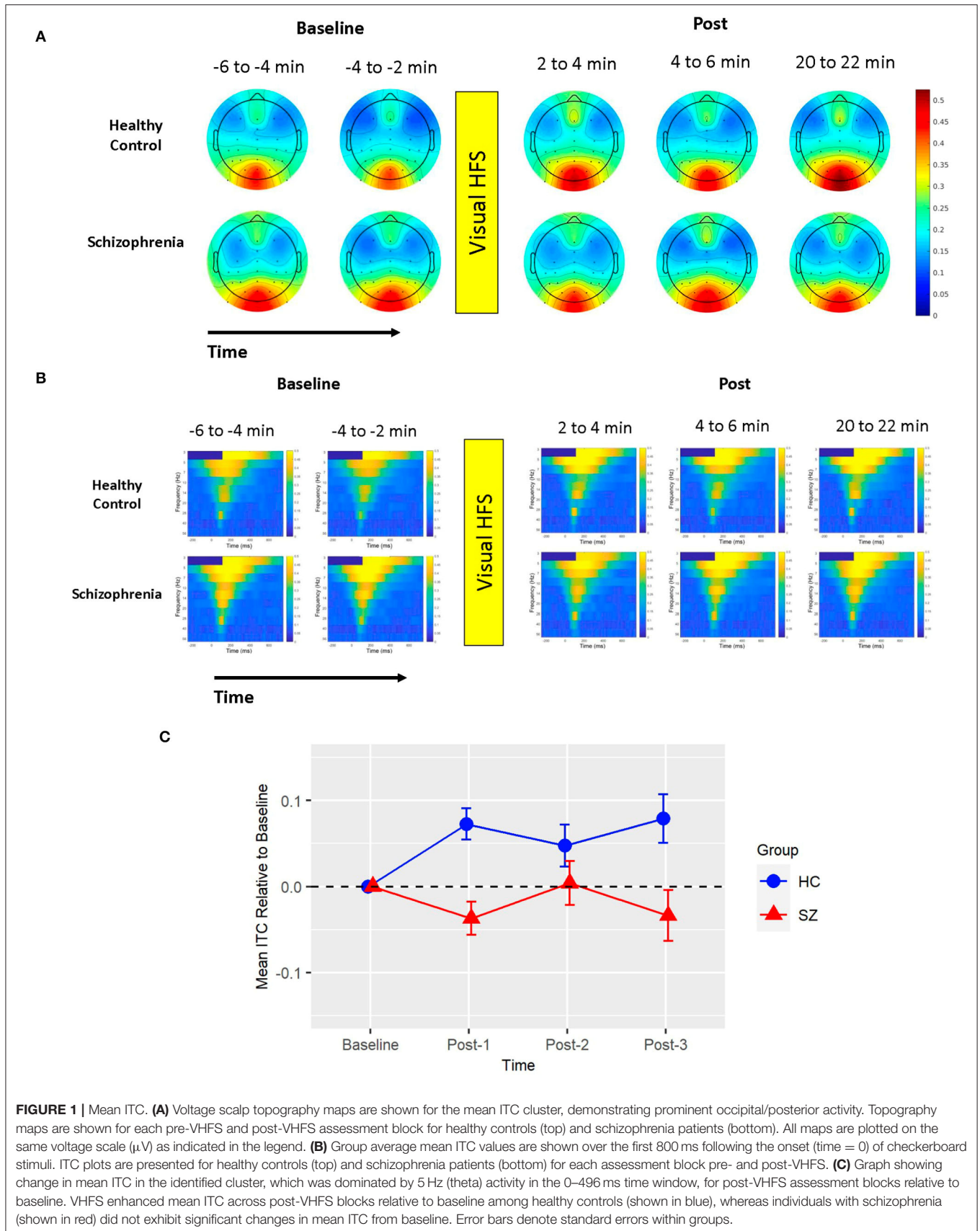
TABLE 1 | Participant demographics and clinical characteristics.

	Schizophrenia (n = 19)	Healthy controls (n = 21)	p-value
Age (years), *Mean (SD)*	40.0 (13.5)	37.9 (13.6)	0.628
Gender			0.527
Male	16	16	
Female	3	5	
Education (years), *Mean (SD)*	13.0 (1.5)	16.1 (3.2)	0.0004
Parental SES[a], *Mean (SD)*	37.3 (16.5)	34.5 (15.0)	0.572
Illness Duration (years), *Mean (SD)*	16.3 (11.6)		
PANSS Score, *Mean (SD)*	57.1 (9.9)		
Total			
Negative	14.8 (8.5)		
Positive	13.7 (8.2)		
General Psychopathology	28.7 (14.9)		
Antipsychotic Dosage[b] (mg), *Mean (SD)*	421.5 (426.6)		

SD, standard deviation; SES, socioeconomic status; PANSS, Positive and Negative Syndrome Scale.
[a]*Hollingshead Scale of Socioeconomic Status; smaller scores indicate higher parental SES.*
[b]*Reported in chlorpromazine equivalent dosages; all schizophrenia participants but one were treated with atypical antipsychotic medications.*
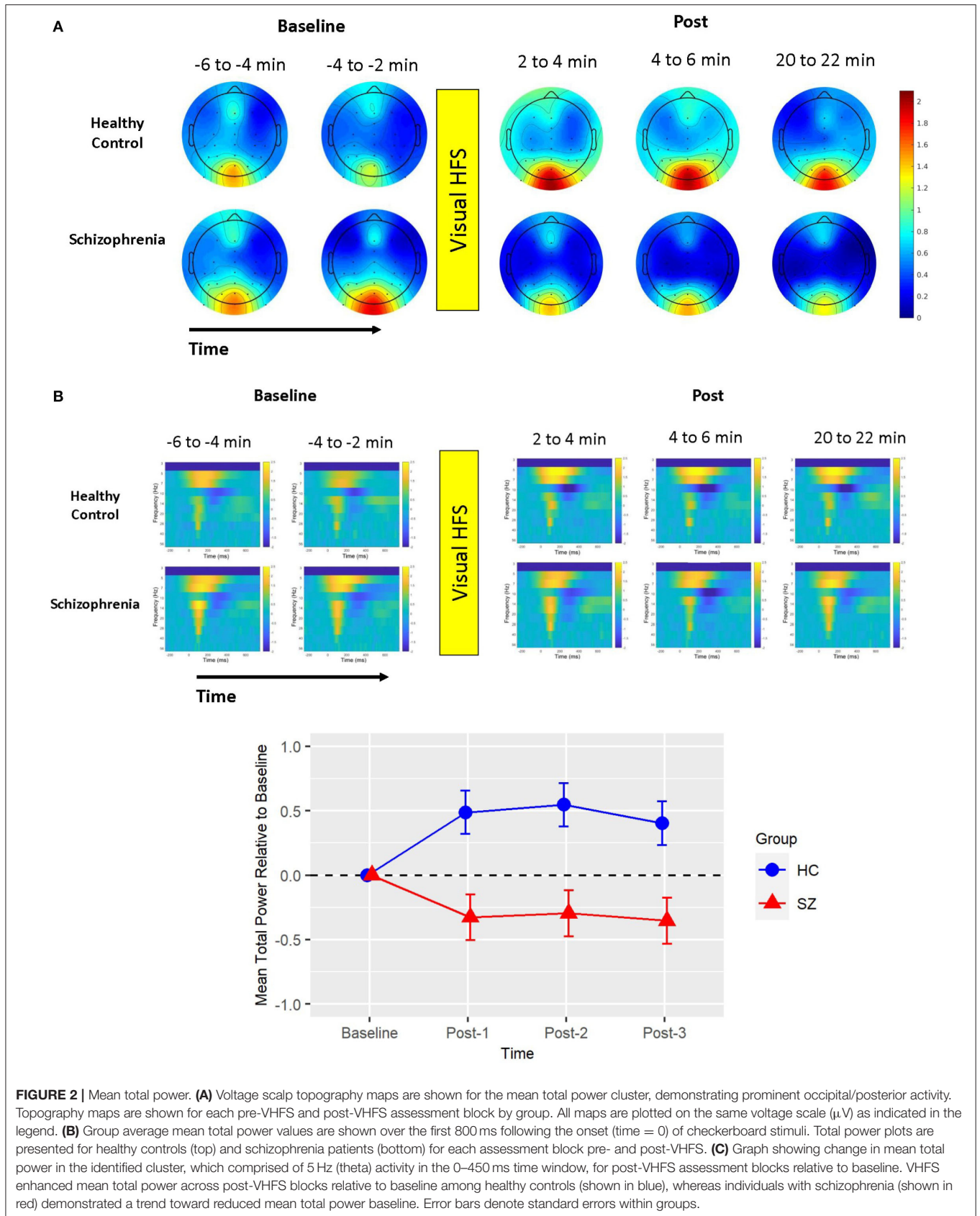
FIGURE 1 | Mean ITC. (A) Voltage scalp topography maps are shown for the mean ITC cluster, demonstrating prominent occipital/posterior activity. Topography maps are shown for each pre-VHFS and post-VHFS assessment block for healthy controls (top) and schizophrenia patients (bottom). All maps are plotted on the same voltage scale (µV) as indicated in the legend. (B) Group average mean ITC values are shown over the first 800 ms following the onset (time = 0) of checkerboard stimuli. ITC plots are presented for healthy controls (top) and schizophrenia patients (bottom) for each assessment block pre- and post-VHFS. (C) Graph showing change in mean ITC in the identified cluster, which was dominated by 5 Hz (theta) activity in the 0–496 ms time window, for post-VHFS assessment blocks relative to baseline. VHFS enhanced mean ITC across post-VHFS blocks relative to baseline among healthy controls (shown in blue), whereas individuals with schizophrenia (shown in red) did not exhibit significant changes in mean ITC from baseline. Error bars denote standard errors within groups.

FIGURE 2 | Mean total power. **(A)** Voltage scalp topography maps are shown for the mean total power cluster, demonstrating prominent occipital/posterior activity. Topography maps are shown for each pre-VHFS and post-VHFS assessment block by group. All maps are plotted on the same voltage scale (μV) as indicated in the legend. **(B)** Group average mean total power values are shown over the first 800 ms following the onset (time = 0) of checkerboard stimuli. Total power plots are presented for healthy controls (top) and schizophrenia patients (bottom) for each assessment block pre- and post-VHFS. **(C)** Graph showing change in mean total power in the identified cluster, which comprised of 5 Hz (theta) activity in the 0–450 ms time window, for post-VHFS assessment blocks relative to baseline. VHFS enhanced mean total power across post-VHFS blocks relative to baseline among healthy controls (shown in blue), whereas individuals with schizophrenia (shown in red) demonstrated a trend toward reduced mean total power baseline. Error bars denote standard errors within groups.

TABLE 2 | Mean (M) and standard deviation (SD) of ITC cluster, total power cluster, and alpha ERD values by group.

	Schizophrenia (n = 19)		Healthy controls (n = 21)	
	M (SD)	Cohen's d	M (SD)	Cohen's d
MEAN ITC				
Baseline	0.35 (0.15)		0.27 (0.09)	
Post-1	0.34 (0.14)	−0.39	0.34 (0.12)	0.87
Post-2	0.35 (0.15)	0.03	0.32 (0.12)	0.43
Post-3	0.32 (0.14)	−0.26	0.35 (0.08)	0.62
MEAN TOTAL POWER				
Baseline	1.06 (0.86)		0.74 (0.55)	
Post-1	0.73 (1.16)	−0.42	1.23 (0.56)	0.63
Post-2	0.76 (0.92)	−0.38	1.29 (0.59)	0.70
Post-3	0.70 (0.98)	−0.45	1.14 (0.56)	0.52
MEAN ALPHA ERD				
Baseline	−0.44 (2.10)		−0.87 (1.54)	
Post-1	−0.63 (2.42)	−0.11	−1.38 (2.19)	−0.30
Post-2	−1.25 (2.37)	−0.44	−1.66 (2.25)	−0.43
Post-3	−0.46 (2.49)	−0.01	−1.52 (2.34)	−0.33

Cohen's d effect size estimates are reported for change from Baseline within group.

In contrast, schizophrenia patients showed no significant changes in mean ITC from baseline to Post-VHFS assessments (Post-1: $p = 0.092$, Post-2: $p = 0.879$, Post-3: $p = 0.257$). Relative to Baseline, mean ITC was significantly enhanced in HC relative to schizophrenia patients for Post-1 ($p = 0.0001$) but not Post-2 ($p = 0.220$). As expected, mean ITC was also significantly enhanced in HC relative to schizophrenia patients for Post-3 ($p = 0.006$).

Total Power Cluster

Mean total power did not differ between Baseline-1 and Baseline-2 in schizophrenia patients ($p = 0.57$) or in HCs ($p = 0.18$), so the baseline blocks were averaged for each participant. Mean total power at Baseline did not significantly differ between groups ($p = 0.21$). As expected from the analysis by which the cluster was identified, the mixed model of mean total power showed a significant Group X Time interaction [$F_{(3,114)} = 5.39$, $p < 0.002$] (see **Figure 2**). In HCs, VHFS enhanced mean total power at all post-VHFS blocks relative to Baseline (Post-1: $p = 0.005$; Post-2: $p = 0.002$; Post-3: $p = 0.019$). In contrast, schizophrenia patients showed a trend toward reduced mean total power from Baseline to post-VHFS blocks (Post-1: $p = 0.070$; Post-2: $p = 0.10$; Post-3: $p = 0.050$). Relative to Baseline, mean total power was significantly enhanced in HC relative to schizophrenia patients for Post-1 ($p = 0.001$) and Post-2 ($p = 0.0009$). As expected, mean total power was also significantly enhanced in HC relative to schizophrenia patients for Post-3 ($p = 0.003$).

Associations With VEP Change Scores

Separate models were used to assess the relationship between (1) the ITC cluster mean and (2) the total power cluster mean and N1b VEP factor scores from our previous report (45). All of these variables were change scores calculated as the difference between Post-3 and the average Baseline assessment. Neither ITC nor total power models showed any evidence of a group difference in the relationship between the cluster and N1b change scores (i.e., no Group X N1b change score interactions, $ps > 0.375$). Reduced models included the N1b change scores and a Group factor, but tests of the common slope (estimated within groups) failed to show N1b change scores to be related to either ITC [$t_{(37)} = 0.274$, $p = 0.78$] or total power [$t_{(37)} = 0.769$, $p = 0.45$] cluster change scores.

Associations With VHFS-Driven VSSR Power

The same GLM framework was used to assess the relationship between ITC and total power mean cluster change scores and VHFS-driven EEG power at ∼8.87 Hz, which was previously shown to predict the LTP-like change in N1b VEP factor scores in HC (45). Like the N1b models previously described, there were no group differences in these relationships, and the common slope across groups failed to show significant relationships between VHFS-driven power and cluster change scores for either ITC or total power (all $ps > 0.08$).

Alpha ERD

Based on the BIC fit statistics, an unstructured variance-covariance structure was the best choice for the alpha ERD model. Alpha ERD did not differ between Baseline-1 and Baseline-2 in patients ($p = 0.62$) or in HCs ($p = 0.73$), and it did not differ between groups at Baseline [collapsed across both assessment blocks ($p = 0.45$)]. There was neither a Group X Time interaction [$F_{(3,38)} = 2.14$, $p = 0.11$] nor a main effect of Group [$F_{(1,38)} = 1.06$, $p = 0.31$] (see **Figure 3**). However, there was a significant effect of Time [$F_{(3,38)} = 6.82$, $p = 0.0009$]. Relative to Baseline, alpha ERD showed an enhancement that reached statistical significance for Post-2 ($p = 0.009$), but not Post-1 ($p = 0.20$), or Post-3 ($p = 0.29$). Of note, a contrast of all Baseline vs. all post-VHFS blocks was marginally significant ($p = 0.08$), indicating a trend toward overall increase in alpha ERD following VHFS.

DISCUSSION

The current EEG time-frequency domain analysis of data from our previously published EEG-based VEP plasticity study (45) examined neuroplastic changes in EEG oscillatory activity induced by a LTP-like visual sensory stimulation paradigm in healthy individuals and in patients with schizophrenia. Using a cluster-based permutation testing approach (65), we found that the delivery of repetitive high frequency visual stimulation (VHFS) induced LTP-like visual cortical potentiation in healthy individuals. This was evident as an increase in visual event-related EEG theta band total power and phase synchrony (ITC) over posterior scalp electrodes from pre- to post-VHFS, plasticity effects that persisted for at least 22 min post-VHFS. Moreover, these plasticity effects were significantly reduced in patients with schizophrenia relative to healthy individuals; indeed, patients did not show significant increases in theta power or ITC from baseline to post-VHFS for any of the post-VHFS assessment blocks.
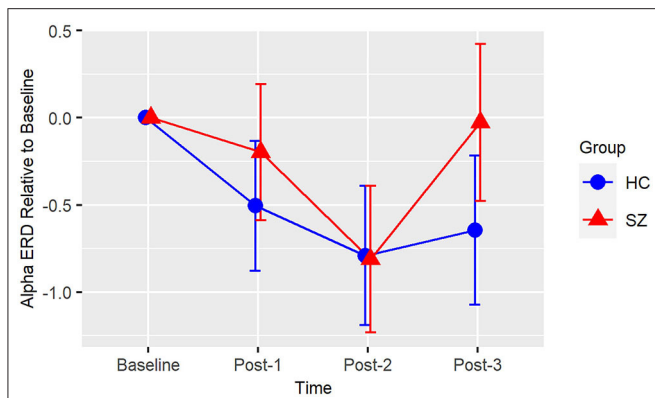
FIGURE 3 | Alpha ERD. Graph showing change in alpha ERD for post-VHFS assessment blocks relative to baseline. Alpha ERD showed a trend toward overall enhancement post-VHFS relative to baseline; specifically, this enhancement reached statistical significance for Post-2 but not Post-1 or Post-3 across healthy control participants (shown in blue) and schizophrenia patients (shown in red). Groups did not differ in alpha ERD potentiation post-VHFS. Error bars denote standard errors within groups.

Consistent with our prior analysis showing VHFS-induced LTP-like plasticity impairments in schizophrenia using VEPs (45), the present time-frequency analysis of EEG oscillatory activity provides further evidence of compromised visual LTP-like plasticity in patients with schizophrenia. Importantly, these results are not consistent with a more recent study using a different visual cortical plasticity paradigm in which a stimulus-specific (analogous to "input specificity" in LTP) VEP plasticity effect was demonstrated and found to be intact in schizophrenia patients (44). However, they are broadly consistent with other studies showing schizophrenia patients to have LTP-like auditory plasticity deficits using a high frequency auditory stimulation paradigm (48) and motor plasticity deficits using transcranial magnetic stimulation [see (78)] and transcranial direct current stimulation [see (79)] plasticity induction paradigms. This observed LTP-like plasticity deficit in schizophrenia may be a consequence NMDAR hypofunction, which in turn may arise from schizophrenia risk genes (13, 80, 81). LTP-like cortical plasticity was recently shown to be enhanced by a glycine transporter-1 inhibitor, presumably by co-agonism of glycine at the NMDAR site (47), while another recent study showed d-cycloserine, which also modulates NMDAR function, to enhance LTP-like plasticity in healthy individuals (46) but not in patients with schizophrenia (3). Furthermore, plasticity deficits in schizophrenia have been shown to correlate with neurocognitive deficits (82). These VHFS plasticity studies, which all used the Cavus et al. (45) paradigm analyzed in the present study, are broadly consistent with NMDAR-dependent plasticity deficits in schizophrenia. Given the few studies (3, 47) and mixed findings, it remains unclear whether plasticity deficits as assessed by sensory LTP-like plasticity paradigms can be pharmacologically rescued via augmentation of NMDAR neurotransmission in patients with schizophrenia.

Importantly, the VHFS-induced neuro-oscillatory plasticity effects, and their deficits in schizophrenia patients, identified by cluster-based permutation analysis of the EEG time-frequency data pre- and post-VHFS were primarily limited to the theta band for both total power and ITC measures. Theta oscillations have been observed across several cortical regions, including in the hippocampus as well as prefrontal, somatosensory, and visual cortices [see (83–85)], and are thought to depend primarily on the interplay between cortical pyramidal neurons and somatostatin (SST)-type GABAergic interneurons (86, 87). Critically, theta oscillations have been implicated in synaptic plasticity (54, 59, 60, 88, 89) and in learning and memory [e.g., (63, 90–94)], and reduced amplitude of theta oscillations during both memory and executive function tasks have been observed in schizophrenia (95, 96). Importantly, recent work in schizophrenia has mapped auditory plasticity deficits, including impaired mismatch negativity (MMN) and N100 generation during paired tone matching, to alterations in the theta frequency band (97–101). Such deficits during tone matching have been shown to predict higher-order impairments in working memory, reading, and emotion recognition (102). Moreover, theta band abnormalities underlying auditory MMN deficits, which have been shown to be modulated by glutamatergic NMDAR drug manipulations in schizophrenia (103, 104), are correlated with executive functions, including working memory (100, 105), as well as non-verbal memory and social cognition (100) in patients with schizophrenia.

LTP in particular in hippocampal recordings of rats *in vivo* has been shown to depend on suppression of theta band power during high frequency tetanization as well as subsequent increases in theta power above pre-tetanization baseline levels during the first 5 min following tetanization (59, 60). Rats showing these increases exhibited successful LTP that persisted for over 24 h (59, 60). In contrast, no concurrent suppression of theta power during tetanization nor enhancement of theta power in the immediate aftermath of tetanization was observed in rats that failed to show LTP (59, 60). Our results are highly consistent with this animal work and suggest that a transient increase in theta oscillations following VHFS may be necessary for the processing of sensory input during VHFS and for successful LTP, allowing for the formation of a memory trace of recently acquired sensory information (60). Moreover, in a rodent model of psychosis, in which rats were treated with the NMDAR antagonist MK801 resulting in significant and chronic deficits in LTP and spatial memory, Kalweit et al. (27) observed a suppression of 5 Hz hippocampal theta power for 300 s post-tetanization relative to control rats not treated with MK801. Similarly, we report a reduction of 5 Hz theta power below that of pre-VHFS baseline in schizophrenia patients that endured over the three post-VHFS blocks. Taken together, these results implicate altered theta oscillations in deficient NMDAR-dependent LTP-like visual plasticity in schizophrenia that may contribute to downstream impairments in learning, memory, and cognitive function.

The rodent studies described above have also shown that theta-gamma phase-amplitude coupling *during* high frequency

tetanization predicts successful LTP 24 h post-tetanus, and that uncoupling of theta-gamma oscillations during tetanization is evident following interventions that disrupt LTP (106), including MK801-induced NMDA hypofunction (27). In rats, gamma oscillations were not disrupted by MK801 treatment, suggesting that the observed change in theta-gamma coupling likely derived from changes in theta activity during the tetanization. In these rodent studies, successful *in vivo* hippocampal LTP was associated with suppression of theta power relative to baseline during the first half of the tetanization period, and beginning in the second half, an increase in theta power that rose above baseline levels over the first 200 s post-tetanus. This post-tetanus theta power increase in rats showing successful LTP was also accompanied by a transient increase in gamma power 100 s post-tetanus (59, 60). Interestingly, based on the physiological microcircuitry connecting theta-generating pyramidal neurons and gamma-generating parvalbumin-expressing GABAergic interneurons (107–110), the authors suggest that theta oscillation increases may drive the accompanying increases in gamma oscillations in the period immediately following tetanization that predict successful LTP (59, 60, 111). Taken together, these results suggest that a particular profile of theta-gamma power changes and coupling during and immediately after high frequency tetanizing stimulation is required for successful hippocampal LTP induction. Translating and extrapolating from these basic neuroscience LTP studies, future research examining human LTP-like visual cortical plasticity induced by sensory stimulation should examine theta and gamma oscillatory activity during and immediately following VHFS to determine if power changes and cross-frequency coupling predict successful LTP in humans in a manner similar to the profile described in successful hippocampal LTP in rats. Furthermore, future studies should examine whether deficiencies in specific elements of this theta-gamma activity profile during and immediately following VHFS can account for deficient LTP-like plasticity in schizophrenia. The fact that acute and sub-chronic treatment with the NMDAR antagonist MK801 disrupted LTP and weakened theta-gamma coupling and power increases during and immediately following high frequency tetanization (27) is consistent with the possible role of NMDAR hypofunction in mediating deficient theta power and phase synchrony increases immediately following VHFS in the patients with schizophrenia in our study. Based on the rodent work, this early theta increase, which persisted out to 22 min in the HC subjects in our study, may be necessary for successful VHFS-induction of LTP-like visual cortical plasticity.

Interestingly, the magnitudes of the theta band plasticity effects we observed were not associated with the degree of N1b VEP potentiation we reported previously (45), suggesting that plasticity shown by evoked potentials and theta oscillations reflect changes in distinct aspects of the neural machinery subserving visual cortical information processing. It may be the case that VEPs, such as the N1b, provide a more direct index of plasticity among primary visual cortex neurons that are spatially tuned to stimulus orientation and contrast features, while theta band measures may reflect longer range cortical communication and connectivity among cortical regions. Future multimodal

imaging (e.g., simultaneous EEG-fMRI) investigations utilizing the cortical plasticity paradigm could clarify the association between theta band oscillations and functional connectivity during and post-VHFS.

In addition, in our prior VEP report, a higher magnitude of the VSSR 8.9 Hz EEG power driven by VHFS predicted greater N1b potentiation in HC, but not in schizophrenia patients (45). The fact that the 8.9 Hz VSSR power during VHFS was equivalent in healthy individuals and schizophrenia patients provided some evidence that differential attention to VHFS, which is known to contribute to variation in VSSR power (112), did not account for the deficits in N1b potentiation we previously reported (45) and similarly does not account for the deficits in theta power and phase synchrony potentiation observed in our current analysis. However, in contrast with the plasticity effects on N1b we previously reported, we did not find evidence of the same link between the degree of theta potentiation and the magnitude of the VSSR in response to VHFS in the healthy group. Neuroplastic changes in theta oscillations may be less dependent on attention-mediated engagement with the high frequency stimulation than the neuroplastic changes induced in VEP component amplitudes.

Consistent with the prior report of Clapp et al. (61), we also showed a small enhancement of visual-stimulus evoked alpha ERD following VHFS. While our post-VHFS assessments occurred over the course of 22 min, Clapp et al. (61) found alpha ERD enhancement over the course of 1 h post-VHFS. However, because we did not conduct post-VHFS assessments beyond 22 min, we were unable to test for the presence of a more enduring potentiation of the alpha ERD effect. Patients with schizophrenia have previously been shown to exhibit reduced alpha ERD, particularly in response to target tones during an auditory oddball task (113). However, baseline alpha ERD to the visual stimuli in the present study were similar in patients and healthy individuals, and unlike the observed deficits in potentiation of theta oscillations, the potentiation of alpha ERD appears to be relatively intact in schizophrenia patients following VHFS. These results suggest that patients with schizophrenia are able to engage their neuronal networks in response to the visual stimulus and that alterations in alpha ERD are not likely to drive deficient LTP in patients.

This study had several limitations. The visual cortical plasticity paradigm we utilized included a shorter post-VHFS follow-up assessment period relative to many of the paradigms previously implemented in healthy individuals. This was due primarily due to our motivation to keep the paradigm as short as possible to mitigate any difficulties patients with schizophrenia may have in tolerating a lengthy EEG testing session. However, as previously noted, prior studies using similar paradigms have demonstrated persistence of VEP potentiation and alpha ERD effects for at least 1 h. In addition, the paradigm we implemented did not include a non-tetanized control stimulus to test for input specificity of potentiation effects; nonetheless, prior studies in both healthy individuals and schizophrenia patients using similar paradigms have shown VEP potentiation that was specific to the tetanized stimulus (39, 40, 43, 44). Moreover, it is possible that antipsychotic medications may have contributed to the

observed plasticity deficits in our schizophrenia sample; future studies should attempt to address this medication confound. Finally, our study was limited in its solitary focus on examining LTP-like plasticity in visual cortex; while such impairments may contribute to visual processing and memory deficits in schizophrenia (114), they are unlikely to account for the full range of schizophrenia symptoms and cognitive impairments. Nonetheless, visual cortical plasticity impairment may reflect more general neuroplasticity dysfunction that affects other sensory modalities and cortices.

In conclusion, our results provide further evidence of deficient LTP-like cortical plasticity in schizophrenia and are consistent with NMDAR hypofunction in the illness. Given our observations of VHFS-induced theta oscillation power changes similar to those observed in rodent studies (27, 59, 60, 111), sensory plasticity paradigms like the visual paradigm employed in our study show considerable promise as a translational bridge between human and animal studies, particularly because identical stimuli can be used to induce LTP in animals (31, 34, 36). Ultimately, paradigms that probe LTP-like plasticity, such as the VHFS paradigm, may provide treatment targets and physiological readouts of treatment outcomes for novel drug development aimed at restoring normal neural plasticity in schizophrenia. Success with plasticity-enhancing treatments may, in turn, set the stage for other cognitive and behavioral treatments that depend on intact mechanisms of plasticity to improve symptoms and cognitive deficits in schizophrenia.

DATA AVAILABILITY STATEMENT

The raw data supporting the conclusions of this article will be made available by the authors, without undue reservation.

ETHICS STATEMENT

The studies involving human participants were reviewed and approved by Yale University and West Haven VA IRBs. The patients/participants provided their written informed consent to participate in this study.

AUTHOR CONTRIBUTIONS

FUNDING

REFERENCES

1. Stephan KE, Baldeweg T, Friston KJ. Synaptic plasticity and dysconnection in schizophrenia. *Biol Psychiatry.* (2006) 59:929–39. doi: 10.1016/j.biopsych.2005.10.005
2. Stephan KE, Friston KJ, Frith CD. Dysconnection in schizophrenia: from abnormal synaptic plasticity to failures of self-monitoring. *Schizophr Bull.* (2009) 35:509–27. doi: 10.1093/schbul/sbn176
3. Forsyth JK, Lewis DA. Mapping the consequences of impaired synaptic plasticity in schizophrenia through development: an integrative model for diverse clinical features. *Trends Cogn Sci.* (2017) 21:760–78. doi: 10.1016/j.tics.2017.06.006
4. Green MF. What are the functional consequences of neurocognitive deficits in schizophrenia? *Am J Psychiatry.* (1996) 153:321–30. doi: 10.1176/ajp.153.3.321
5. Green MF, Kern RS, Braff DL, Mintz J. Neurocognitive deficits and functional outcome in schizophrenia: are we measuring the "right stuff"? *Schizophr Bull.* (2000) 26:119–36. doi: 10.1093/oxfordjournals.schbul.a033430
6. Bliss TV, Collingridge GL. A synaptic model of memory: long-term potentiation in the hippocampus. *Nature.* (1993) 361:31–9. doi: 10.1038/361031a0
7. Cooke SF, Bliss TV. Plasticity in the human central nervous system. *Brain.* (2006) 129:1659–73. doi: 10.1093/brain/awl082
8. Malenka RC, Nicoll RA. Long-term potentiation–a decade of progress? *Science.* (1999) 285:1870–4. doi: 10.1126/science.285.5435.1870
9. Citri A, Malenka RC. Synaptic plasticity: multiple forms, functions, and mechanisms. *Neuropsychopharmacology.* (2008) 33:18–41. doi: 10.1038/sj.npp.1301559
10. Feldman DE. Synaptic mechanisms for plasticity in neocortex. *Annu Rev Neurosci.* (2009) 32:33–55. doi: 10.1146/annurev.neuro.051508.135516
11. Bliss TV, Cooke SF. Long-term potentiation and long-term depression: a clinical perspective. *Clinics.* (2011) 66(Suppl.1):3–17. doi: 10.1590/S1807-59322011001300002
12. Ho VM, Lee JA, Martin KC. The cell biology of synaptic plasticity. *Science.* (2011) 334:623–8. doi: 10.1126/science.1209236
13. Harrison PJ, Weinberger DR. Schizophrenia genes, gene expression, and neuropathology: on the matter of their convergence. *Mol Psychiatry.* (2005) 10:40–68. doi: 10.1038/sj.mp.4001558
14. Javitt DC, Zukin SR, Heresco-Levy U, Umbricht D. Has an angel shown the way? Etiological and therapeutic implications of the PCP/NMDA model of schizophrenia. *Schizophr Bull.* (2012) 38:958–66. doi: 10.1093/schbul/sbs069
15. Moghaddam B, Javitt D. From revolution to evolution: the glutamate hypothesis of schizophrenia and its implication for treatment. *Neuropsychopharmacology.* (2012) 37:4–15. doi: 10.1038/npp.2011.181
16. Moghaddam B, Krystal JH. Capturing the angel in "angel dust:" 20 years of translational neuroscience studies of NMDA receptor antagonists in animals and humans. *Schizophr Bull.* (2012) 38:942–9. doi: 10.1093/schbul/sbs075
17. Catts VS, Lai YL, Weickert CS, Weickert TW, Catts SV. A quantitative review of the postmortem evidence for decreased cortical N-methyl-D-aspartate receptor expression levels in schizophrenia: how can we link molecular

abstractnormalities to mismatch negativity deficits? *Biol Psychol.* (2016) 116:57–67. doi: 10.1016/j.biopsycho.2015.10.013

18. Pilowsky LS, Bressan RA, Stone JM, Erlandsson K, Mulligan RS, Krystal JH, et al. First *in vivo* evidence of an NMDA receptor deficit in medication-free schizophrenic patients. *Mol Psychiatry.* (2006) 11:118–9. doi: 10.1038/sj.mp.4001751

19. Coyle JT, Tsai G, Goff D. Converging evidence of NMDA receptor hypofunction in the pathophysiology of schizophrenia. *Ann N Y Acad Sci.* (2003) 1003:318–27. doi: 10.1196/annals.1300.020

20. Coyle JT, Tsai G. NMDA receptor function, neuroplasticity, and the pathophysiology of schizophrenia. *Int Rev Neurobiol.* (2004) 59:491–515. doi: 10.1016/S0074-7742(04)59019-0

21. Haracz JL. Neural plasticity in schizophrenia. *Schizophr Bull.* (1985) 11:191–229. doi: 10.1093/schbul/11.2.191

22. Mccullumsmith RE, Clinton SM, Meador-Woodruff JH. Schizophrenia as a disorder of neuroplasticity. *Int Rev Neurobiol.* (2004) 59:19–45. doi: 10.1016/S0074-7742(04)59002-5

23. Lips ES, Cornelisse LN, Toonen RF, Min JL, Hultman CM, International Schizophrenia C, et al. Functional gene group analysis identifies synaptic gene groups as risk factor for schizophrenia. *Mol Psychiatry.* (2012) 17:996–1006. doi: 10.1038/mp.2011.117

24. Schizophrenia Working Group of the Psychiatric Genomics C. Biological insights from 108 schizophrenia-associated genetic loci. *Nature.* (2014) 511:421–7. doi: 10.1038/nature13595

25. Lau CG, Zukin RS. NMDA receptor trafficking in synaptic plasticity and neuropsychiatric disorders. *Nat Rev Neurosci.* (2007) 8:413–26. doi: 10.1038/nrn2153

26. Manahan-Vaughan D, Wildforster V, Thomsen C. Rescue of hippocampal LTP and learning deficits in a rat model of psychosis by inhibition of glycine transporter-1 (GlyT1). *Eur J Neurosci.* (2008) 28:1342–50. doi: 10.1111/j.1460-9568.2008.06433.x

27. Kalweit AN, Amanpour-Gharaei B, Colitti-Klausnitzer J, Manahan-Vaughan D. Changes in neuronal oscillations accompany the loss of hippocampal LTP that occurs in an animal model of psychosis. *Front Behav Neurosci.* (2017) 11:36. doi: 10.3389/fnbeh.2017.00036

28. Selemon LD, Goldman-Rakic PS. The reduced neuropil hypothesis: a circuit based model of schizophrenia. *Biol Psychiatry.* (1999) 45:17–25. doi: 10.1016/S0006-3223(98)00281-9

29. Glausier JR, Lewis DA. Dendritic spine pathology in schizophrenia. *Neuroscience.* (2013) 251:90–107. doi: 10.1016/j.neuroscience.2012.04.044

30. Ganguly K, Poo MM. Activity-dependent neural plasticity from bench to bedside. *Neuron.* (2013) 80:729–41. doi: 10.1016/j.neuron.2013.10.028

31. Clapp WC, Eckert MJ, Teyler TJ, Abraham WC. Rapid visual stimulation induces N-methyl-D-aspartate receptor-dependent sensory long-term potentiation in the rat cortex. *Neuroreport.* (2006) 17:511–5. doi: 10.1097/01.wnr.0000209004.63352.10

32. Frenkel MY, Sawtell NB, Diogo AC, Yoon B, Neve RL, Bear MF. Instructive effect of visual experience in mouse visual cortex. *Neuron.* (2006) 51:339–49. doi: 10.1016/j.neuron.2006.06.026

33. Cooke SF, Bear MF. Visual experience induces long-term potentiation in the primary visual cortex. *J Neurosci.* (2010) 30:16304–13. doi: 10.1523/JNEUROSCI.4333-10.2010

34. Cooke SF, Bear MF. Stimulus-selective response plasticity in the visual cortex: an assay for the assessment of pathophysiology and treatment of cognitive impairment associated with psychiatric disorders. *Biol Psychiatry.* (2012) 71:487–95. doi: 10.1016/j.biopsych.2011.09.006

35. Kirk IJ, Mcnair NA, Hamm JP, Clapp WC, Mathalon DH, Cavus I, et al. Long-term potentiation (LTP) of human sensory-evoked potentials. *Wiley Interdiscip Rev Cogn Sci.* (2010) 1:766–73. doi: 10.1002/wcs.62

36. Clapp WC, Hamm JP, Kirk IJ, Teyler TJ. Translating long-term potentiation from animals to humans: a novel method for non-invasive assessment of cortical plasticity. *Biol Psychiatry.* (2012) 71:496–502. doi: 10.1016/j.biopsych.2011.08.021

37. Clapp WC, Kirk IJ, Hamm JP, Shepherd D, Teyler TJ. Induction of LTP in the human auditory cortex by sensory stimulation. *Eur J Neurosci.* (2005) 22:1135–40. doi: 10.1111/j.1460-9568.2005.04293.x

38. Teyler TJ, Hamm JP, Clapp WC, Johnson BW, Corballis MC, Kirk IJ. Long-term potentiation of human visual evoked responses. *Eur J Neurosci.* (2005) 21:2045–50. doi: 10.1111/j.1460-9568.2005.04007.x

39. Ross RM, Mcnair NA, Fairhall SL, Clapp WC, Hamm JP, Teyler TJ, et al. Induction of orientation-specific LTP-like changes in human visual evoked potentials by rapid sensory stimulation. *Brain Res Bull.* (2008) 76:97–101. doi: 10.1016/j.brainresbull.2008.01.021

40. Mcnair NA, Clapp WC, Hamm JP, Teyler TJ, Corballis MC, Kirk IJ. Spatial frequency-specific potentiation of human visual-evoked potentials. *Neuroreport.* (2006) 17:739–41. doi: 10.1097/01.wnr.0000215775.53732.9f

41. Clapp WC, Zaehle T, Lutz K, Marcar VL, Kirk IJ, Hamm JP, et al. Effects of long-term potentiation in the human visual cortex: a functional magnetic resonance imaging study. *Neuroreport.* (2005) 16:1977–80. doi: 10.1097/00001756-200512190-00001

42. Lahr J, Peter J, Bach M, Mader I, Nissen C, Normann C, et al. Heterogeneity of stimulus-specific response modification-an fMRI study on neuroplasticity. *Front Hum Neurosci.* (2014) 8:695. doi: 10.3389/fnhum.2014.00695

43. Beste C, Wascher E, Gunturkun O, Dinse HR. Improvement and impairment of visually guided behavior through LTP- and LTD-like exposure-based visual learning. *Curr Biol.* (2011) 21:876–82. doi: 10.1016/j.cub.2011.03.065

44. Wynn JK, Roach BJ, Mccleery A, Marder SR, Mathalon DH, Green MF. Evaluating visual neuroplasticity with EEG in schizophrenia outpatients. *Schizophr Res.* (2019) 212:40–6. doi: 10.1016/j.schres.2019.08.015

45. Cavus I, Reinhart RM, Roach BJ, Gueorguieva R, Teyler TJ, Clapp WC, et al. Impaired visual cortical plasticity in schizophrenia. *Biol Psychiatry.* (2012) 71:512–20. doi: 10.1016/j.biopsych.2012.01.013

46. Forsyth JK, Bachman P, Mathalon DH, Roach BJ, Asarnow RF. Augmenting NMDA receptor signaling boosts experience-dependent neuroplasticity in the adult human brain. *Proc Natl Acad Sci USA.* (2015) 112:15331–6. doi: 10.1073/pnas.1509262112

47. D'souza DC, Carson RE, Driesen N, Johannesen J, Ranganathan M, Krystal JH, et al. Dose-related target occupancy and effects on circuitry, behavior, and neuroplasticity of the glycine transporter-1 inhibitor PF-03463275 in healthy and schizophrenia subjects. *Biol Psychiatry.* (2018) 84:413–21. doi: 10.1016/j.biopsych.2017.12.019

48. Mears RP, Spencer KM. Electrophysiological assessment of auditory stimulus-specific plasticity in schizophrenia. *Biol Psychiatry.* (2012) 71:503–11. doi: 10.1016/j.biopsych.2011.12.016

49. Elvsashagen T, Moberget T, Boen E, Boye B, Englin NO, Pedersen PO, et al. Evidence for impaired neocortical synaptic plasticity in bipolar II disorder. *Biol Psychiatry.* (2012) 71:68–74. doi: 10.1016/j.biopsych.2011.09.026

50. Elvsashagen T. Longitudinal and Cross-Sectional Investigations of LTP-Like Cortical Plasticity in Healthy Individuals and Subjects With Bipolar Disorder Type II. In: *American College of Nueropsychopharmacology 56th Annual meeting.* Palm Springs, CA. (2017).

51. Zak N, Moberget T, Boen E, Boye B, Waage TR, Dietrichs E, et al. Longitudinal and cross-sectional investigations of long-term potentiation-like cortical plasticity in bipolar disorder type II and healthy individuals. *Transl Psychiatry.* (2018) 8:103. doi: 10.1038/s41398-018-0151-5

52. Normann C, Schmitz D, Furmaier A, Doing C, Bach M. Long-term plasticity of visually evoked potentials in humans is altered in major depression. *Biol Psychiatry.* (2007) 62:373–80. doi: 10.1016/j.biopsych.2006.10.006

53. Pavlides C, Greenstein YJ, Grudman M, Winson J. Long-term potentiation in the dentate gyrus is induced preferentially on the positive phase of theta-rhythm. *Brain Res.* (1988) 439:383–7. doi: 10.1016/0006-8993(88)91499-0

54. Huerta PT, Lisman JE. Heightened synaptic plasticity of hippocampal CA1 neurons during a cholinergically induced rhythmic state. *Nature.* (1993) 364:723–5. doi: 10.1038/364723a0

55. Singer W, Gray CM. Visual feature integration and the temporal correlation hypothesis. *Annu Rev Neurosci.* (1995) 18:555–86. doi: 10.1146/annurev.ne.18.030195.003011

56. Wespatat V, Tennigkeit F, Singer W. Phase sensitivity of synaptic modifications in oscillating cells of rat visual cortex. *J Neurosci.* (2004) 24:9067–75. doi: 10.1523/JNEUROSCI.2221-04.2004

57. Ford JM, Krystal JH, Mathalon DH. Neural synchrony in schizophrenia: from networks to new treatments. *Schizophr Bull.* (2007) 33:848–52. doi: 10.1093/schbul/sbm062

58. Uhlhaas PJ, Singer W. Abnormal neural oscillations and synchrony in schizophrenia. *Nat Rev Neurosci.* (2010) 11:100–13. doi: 10.1038/nrn2774

59. Bikbaev A, Manahan-Vaughan D. Hippocampal network activity is transiently altered by induction of long-term potentiation in the dentate gyrus of freely behaving rats. *Front Behav Neurosci.* (2007) 1:7. doi: 10.3389/neuro.08.007.2007

60. Bikbaev A, Manahan-Vaughan D. Relationship of hippocampal theta and gamma oscillations to potentiation of synaptic transmission. *Front Neurosci.* (2008) 2:56–63. doi: 10.3389/neuro.01.010.2008

61. Clapp WC, Muthukumaraswamy SD, Hamm JP, Teyler TJ, Kirk IJ. Long-term enhanced desynchronization of the alpha rhythm following tetanic stimulation of human visual cortex. *Neurosci Lett.* (2006) 398:220–3. doi: 10.1016/j.neulet.2005.12.081

62. Pfurtscheller G, Stancak AJr, Neuper C. Event-related synchronization (ERS) in the alpha band–an electrophysiological correlate of cortical idling: a review. *Int J Psychophysiol.* (1996) 24:39–46. doi: 10.1016/S0167-8760(96)00066-9

63. Klimesch W, Sauseng P, Hanslmayr S. EEG alpha oscillations: the inhibition-timing hypothesis. *Brain Res Rev.* (2007) 53:63–88. doi: 10.1016/j.brainresrev.2006.06.003

64. Delorme A, Makeig S. EEGLAB: an open source toolbox for analysis of single-trial EEG dynamics including independent component analysis. *J Neurosci Methods.* (2004) 134:9–21. doi: 10.1016/j.jneumeth.2003.10.009

65. Maris E, Oostenveld R. Nonparametric statistical testing of EEG- and MEG-data. *J Neurosci Methods.* (2007) 164:177–90. doi: 10.1016/j.jneumeth.2007.03.024

66. Tallon-Baudry C, Bertrand O, Delpuech C, Permier J. Oscillatory gamma-band (30–70 Hz) activity induced by a visual search task in humans. *J Neurosci.* (1997) 17:722–34. doi: 10.1523/JNEUROSCI.17-02-00722.1997

67. First MB, Gibbon M, Williams JBW. *Structured Clinical Interview for DSM-IV Axis I Disorders.* New York, NY: New York State Psychiatric Institute, Biometrics Research Department (1995). doi: 10.1037/t07827-000

68. Kay SR, Fiszbein A, Opler LA. The positive and negative syndrome scale (PANSS) for schizophrenia. *Schizophr Bull.* (1987) 13:261–76. doi: 10.1093/schbul/13.2.261

69. Crovitz HF, Zener K. A group-test for assessing hand- and eye-dominance. *Am J Psychol.* (1962) 75:271–6. doi: 10.2307/1419611

70. Hollingshead AA. *Four-Factor Index of Social Status.* New Haven: Yale University. (1975).

71. Gratton G, Coles MG, Donchin E. A new method for off-line removal of ocular artifact. *Electroencephalogr Clin Neurophysiol.* (1983) 55:468–84. doi: 10.1016/0013-4694(83)90135-9

72. De Clercq W, Vergult A, Vanrumste B, Van Paesschen W, Van Huffel S. Canonical correlation analysis applied to remove muscle artifacts from the electroencephalogram. *IEEE Trans Biomed Eng.* (2006) 53:2583–7. doi: 10.1109/TBME.2006.879459

73. Ries S, Janssen N, Burle B, Alario FX. Response-locked brain dynamics of word production. *PLoS ONE.* (2013) 8:e58197. doi: 10.1371/journal.pone.0058197

74. Kort NS, Ford JM, Roach BJ, Gunduz-Bruce H, Krystal JH, Jaeger J, et al. Role of N-methyl-D-aspartate receptors in action-based predictive coding deficits in schizophrenia. *Biol Psychiatry.* (2017) 81:514–24. doi: 10.1016/j.biopsych.2016.06.019

75. Nolan H, Whelan R, Reilly RB. FASTER: fully automated statistical thresholding for EEG artifact rejection. *J Neurosci Methods.* (2010) 192:152–62. doi: 10.1016/j.jneumeth.2010.07.015

76. Oostenveld R, Fries P, Maris E, Schoffelen JM. FieldTrip: open source software for advanced analysis of MEG, EEG, and invasive electrophysiological data. *Comput Intell Neurosci.* (2011) 2011:156869. doi: 10.1155/2011/156869

77. Schwarz G. Estimating the dimension of a model. *Ann Statist.* (1978) 6:461–4. doi: 10.1214/aos/1176344136

78. Mehta UM, Thanki MV, Padmanabhan J, Pascual-Leone A, Keshavan MS. Motor cortical plasticity in schizophrenia: a meta-analysis of transcranial magnetic stimulation—electromyography studies. *Schizophr Res.* (2019) 207:37–47. doi: 10.1016/j.schres.2018.10.027

79. Hasan A, Nitsche MA, Rein B, Schneider-Axmann T, Guse B, Gruber O, et al. Dysfunctional long-term potentiation-like plasticity in schizophrenia revealed by transcranial direct current stimulation. *Behav Brain Res.* (2011) 224:15–22. doi: 10.1016/j.bbr.2011.05.017

80. Kantrowitz JT, Javitt DC. N-methyl-d-aspartate (NMDA) receptor dysfunction or dysregulation: the final common pathway on the road to schizophrenia? *Brain Res Bull.* (2010) 83:108–21. doi: 10.1016/j.brainresbull.2010.04.006

81. Harrison PJ. Recent genetic findings in schizophrenia and their therapeutic relevance. *J Psychopharmacol.* (2015) 29:85–96. doi: 10.1177/0269881114553647

82. Jahshan C, Wynn JK, Mathalon DH, Green MF. Cognitive correlates of visual neural plasticity in schizophrenia. *Schizophr Res.* (2017) 190:39–45. doi: 10.1016/j.schres.2017.03.016

83. Raghavachari S, Lisman JE, Tully M, Madsen JR, Bromfield EB, Kahana MJ. Theta oscillations in human cortex during a working-memory task: evidence for local generators. *J Neurophysiol.* (2006) 95:1630–8. doi: 10.1152/jn.00409.2005

84. Tsujimoto T, Shimazu H, Isomura Y. Direct recording of theta oscillations in primate prefrontal and anterior cingulate cortices. *J Neurophysiol.* (2006) 95:2987–3000. doi: 10.1152/jn.00730.2005

85. Uhlhaas PJ, Haenschel C, Nikolic D, Singer W. The role of oscillations and synchrony in cortical networks and their putative relevance for the pathophysiology of schizophrenia. *Schizophr Bull.* (2008) 34:927–43. doi: 10.1093/schbul/sbn062

86. Womelsdorf T, Valiante TA, Sahin NT, Miller KJ, Tiesinga P. Dynamic circuit motifs underlying rhythmic gain control, gating and integration. *Nat Neurosci.* (2014) 17:1031–9. doi: 10.1038/nn.3764

87. Hamm JP, Yuste R. Somatostatin interneurons control a key component of mismatch negativity in mouse visual cortex. *Cell Rep.* (2016) 16:597–604. doi: 10.1016/j.celrep.2016.06.037

88. Buzsaki G. Theta oscillations in the hippocampus. *Neuron.* (2002) 33:325–40. doi: 10.1016/S0896-6273(02)00586-X

89. Huerta PT, Lisman JE. Bidirectional synaptic plasticity induced by a single burst during cholinergic theta oscillation in CA1 *in vitro. Neuron.* (1995) 15:1053–63. doi: 10.1016/0896-6273(95)90094-2

90. Lisman JE, Idiart MA. Storage of 7 +/- 2 short-term memories in oscillatory subcycles. *Science.* (1995) 267:1512–5. doi: 10.1126/science.7878473

91. Hasselmo ME. What is the function of hippocampal theta rhythm?–Linking behavioral data to phasic properties of field potential and unit recording data. *Hippocampus.* (2005) 15:936–49. doi: 10.1002/hipo.20116

92. Jones MW, Wilson MA. Theta rhythms coordinate hippocampal-prefrontal interactions in a spatial memory task. *PLoS Biol.* (2005) 3:e402. doi: 10.1371/journal.pbio.0030402

93. Womelsdorf T, Schoffelen JM, Oostenveld R, Singer W, Desimone R, Engel AK, et al. Modulation of neuronal interactions through neuronal synchronization. *Science.* (2007) 316:1609–12. doi: 10.1126/science.1139597

94. Herweg NA, Solomon EA, Kahana MJ. Theta oscillations in human memory. *Trends Cogn Sci.* (2020) 24:208–27. doi: 10.1016/j.tics.2019.12.006

95. Schmiedt C, Brand A, Hildebrandt H, Basar-Eroglu C. Event-related theta oscillations during working memory tasks in patients with schizophrenia and healthy controls. *Brain Res Cogn Brain Res.* (2005) 25:936–47. doi: 10.1016/j.cogbrainres.2005.09.015

96. Haenschel C, Bittner RA, Waltz J, Haertling F, Wibral M, Singer W, et al. Cortical oscillatory activity is critical for working memory as revealed by deficits in early-onset schizophrenia. *J Neurosci.* (2009) 29:9481–9. doi: 10.1523/JNEUROSCI.1428-09.2009

97. Kaser M, Soltesz F, Lawrence P, Miller S, Dodds C, Croft R, et al. Oscillatory underpinnings of mismatch negativity and their relationship

with cognitive function in patients with schizophrenia. *PLoS ONE.* (2013) 8:e83255. doi: 10.1371/journal.pone.0083255

98. Lee M, Sehatpour P, Hoptman MJ, Lakatos P, Dias EC, Kantrowitz JT, et al. Neural mechanisms of mismatch negativity dysfunction in schizophrenia. *Mol Psychiatry.* (2017) 22:1585–93. doi: 10.1038/mp.2017.3

99. Javitt DC, Lee M, Kantrowitz JT, Martinez A. Mismatch negativity as a biomarker of theta band oscillatory dysfunction in schizophrenia. *Schizophr Res.* (2018) 191:51–60. doi: 10.1016/j.schres.2017.06.023

100. Hochberger WC, Joshi YB, Zhang W, Thomas ML, Consortium of Genomics in Schizophrenia I, Braff DL, et al. Decomposing the constituent oscillatory dynamics underlying mismatch negativity generation in schizophrenia: distinct relationships to clinical and cognitive functioning. *Int J Psychophysiol.* (2019) 145:23–9. doi: 10.1016/j.ijpsycho.2018.12.014

101. Javitt DC, Siegel SJ, Spencer KM, Mathalon DH, Hong LE, Martinez A, et al. A roadmap for development of neuro-oscillations as translational biomarkers for treatment development in neuropsychopharmacology. *Neuropsychopharmacology.* (2020) 45:1411–22. doi: 10.1038/s41386-020-0697-9

102. Kantrowitz JT, Epstein ML, Beggel O, Rohrig S, Lehrfeld JM, Revheim N, et al. Neurophysiological mechanisms of cortical plasticity impairments in schizophrenia and modulation by the NMDA receptor agonist D-serine. *Brain.* (2016) 139:3281–95. doi: 10.1093/brain/aww262

103. Swerdlow NR, Bhakta SG, Light GA. Room to move: plasticity in early auditory information processing and auditory learning in schizophrenia revealed by acute pharmacological challenge. *Schizophr Res.* (2018) 199:285–91. doi: 10.1016/j.schres.2018.03.037

104. Kantrowitz JT. N-methyl-d-aspartate-type glutamate receptor modulators and related medications for the enhancement of auditory system plasticity in schizophrenia. *Schizophr Res.* (2019) 207:70–9. doi: 10.1016/j.schres.2018.02.003

105. Xiong YB, Bo QJ, Wang CM, Tian Q, Liu Y, Wang CY. Differential of frequency and duration mismatch negativity and theta power deficits in first-episode and chronic schizophrenia. *Front Behav Neurosci.* (2019) 13:37. doi: 10.3389/fnbeh.2019.00037

106. Bikbaev A, Manahan-Vaughan D. Metabotropic glutamate receptor, mGlu5, regulates hippocampal synaptic plasticity and is required for tetanisation-triggered changes in theta and gamma oscillations. *Neuropharmacology.* (2017) 115:20–9. doi: 10.1016/j.neuropharm.2016.06.004

107. Vida I, Bartos M, Jonas P. Shunting inhibition improves robustness of gamma oscillations in hippocampal interneuron networks by homogenizing firing rates. *Neuron.* (2006) 49:107–17. doi: 10.1016/j.neuron.2005.11.036

108. Fuchs EC, Zivkovic AR, Cunningham MO, Middleton S, Lebeau FE, Bannerman DM, et al. Recruitment of parvalbumin-positive interneurons determines hippocampal function and associated behavior. *Neuron.* (2007) 53:591–604. doi: 10.1016/j.neuron.2007.01.031

109. Lubenov EV, Siapas AG. Hippocampal theta oscillations are travelling waves. *Nature.* (2009) 459:534–9. doi: 10.1038/nature08010

110. Buzsaki G, Wang XJ. Mechanisms of gamma oscillations. *Annu Rev Neurosci.* (2012) 35:203–25. doi: 10.1146/annurev-neuro-062111-150444

111. Kalweit AN, Yang H, Colitti-Klausnitzer J, Fulop L, Bozso Z, Penke B, et al. Acute intracerebral treatment with amyloid-beta (1-42) alters the profile of neuronal oscillations that accompany LTP induction and results in impaired LTP in freely behaving rats. *Front Behav Neurosci.* (2015) 9:103. doi: 10.3389/fnbeh.2015.00103

112. Ding J, Sperling G, Srinivasan R. Attentional modulation of SSVEP power depends on the network tagged by the flicker frequency. *Cereb Cortex.* (2006) 16:1016–29. doi: 10.1093/cercor/bhj044

113. Higashima M, Tsukada T, Nagasawa T, Oka T, Okamoto T, Okamoto Y, et al. Reduction in event-related alpha attenuation during performance of an auditory oddball task in schizophrenia. *Int J Psychophysiol.* (2007) 65:95–102. doi: 10.1016/j.ijpsycho.2007.03.008

114. Silverstein SM, Bakshi S, Nuernberger S, Carpinello K, Wilkniss S. Effects of stimulus structure and target-distracter similarity on the development of visual memory representations in schizophrenia. *Cogn Neuropsychiatry.* (2005) 10:215–29. doi: 10.1080/13546800444000029